Proceedings of the Research Institute of Atmospherics,
Nagoya University, vol. 22 (1975)

8 – CM RADIOHELIOGRAPH

Masato ISHIGURO, Haruo TANAKA, Shinzo ENOME,
Chikayoshi TORII, Yoshio TSUKIJI, Shoji KOBAYASHI
and Naohiko YOSHIMI

Abstract

An 8-cm radioheliograph which has been under construction since 1972 is almost completed. It has a maximum resolving power of 1.5 arc min. and can be operated in various operational modes combined with the existing high-resolution compound interferometer. The minimum time necessary for taking a map is 40 seconds. A two-dimensional mapping will be used whenever necessary by interrupting one-dimensional quick-scanning observations of the radio bursts with the E-W and N-S interferometers. Phase errors in the brightness distributions of the sun can be corrected through computer processing. For the study of active regions, slower scanning modes are available simultaneously with the existing 3-cm radioheliograph. A small computer system with a 32 K words of memory is installed for the scanning control, data acquisition and data processing.

1. Introduction

The radio study of solar flares and active regions has made steady progress with the improvement of the resolving power of antennas. The highest resolution now available in the microwave region is 0.4 arc min. for one-dimensional mapping, which is attained by compound inter-

ferometers at Toyokawa on two different wavelengths, 3 and 8 cm (Tanaka et al. 1967, 1969). The former was completed in 1966 and the latter in 1968. Simultaneous observations with these two instruments have produced valuable information on the spectra of brightness and polarization (Tanaka and Kakinuma 1960, Swarup et al. 1963, Tanaka et al. 1968, Enomé et al. 1969), which are especially useful for the forecasting of proton flares (Tanaka and Kakinuma 1964, Tanaka and Enomé 1975). Furthermore, the quick-scanning operation of the 8-cm interferometer has been a very powerful tool for the study of radio bursts (Tanaka and Enomé 1970, Enomé and Tanaka 1971, 1973). However, the studies with one-dimensional instruments are considerably limited when a source is complicated in structure or when a number of sources are aligned in N-S direction.

As for two-dimensional instruments, or radioheliograph in the microwave region, the Sydney Cross for use on 21 cm with HPBW of 2.4 arc min., and the Stanford Cross for use on 9.1 cm with HPBW of 3.1 arc min. had been in operation until December and August 1973 respectively. The 3-cm radioheliograph at Toyokawa (Tanaka et al. 1970, Arisawa 1971) has the highest resolution of 1.5 arc min., which has been in operation since 1969. A similar radioheliograph on 8 cm was planned prior to the construction of 3-cm radioheliograph, since the simultaneous observations on two different wavelengths had been found absolutely necessary from the study with the one-dimensional interferometers. The outline of the project was already described in 1972 (Ishiguro et al.), when the construction actually started. It took a considerable time to prepare the electronic devices and their adjustments, before the preliminary observations started at the end of 1974.

The 8-cm radioheliograph is composed of T-shaped array of 3-m paraboloids, 32 element in the E-W direction and 17 elements in the N-S direction. The E-W elements are also the main part of the compound interferometer. An additional element is placed at the phase center for the phase error correction developed by Ishiguro (1971, 1974).

One of the remarkable features of this radioheliograph is the easiness in changing the mode and speed of beam scanning for various purposes (Ishiguro et al. 1972). A scanning interferometer with a single pencil beam is very simple in its receiving system, but on the other hand, it has lower time resolution than that of the other image-forming interferometers, such as multi-beam or Fourier-synthesis systems. A simultaneous one-dimensional observation with the E-W and N-S interferometers are very convenient for the purpose of observing the radio bursts. But, the fan-beam scanning in two orthogonal directions does

not give us sufficient information on two-dimensional brightness distribution when a source structure is complicated.

So, it is necessary to prepare various modes of scanning for the different observational purposes. There are five observational modes, the two of which are for the fan-beam scanning and the other three for the pencil-beam scanning. There is also an extra mode for checking the interferometer phase through data processing. To change one operational mode to another, array configuration, driving speed of the phase shifters and data sampling rate must be changed. Two-dimensional scanning at the highest speed produces one map in every 40 seconds. One frame is composed of 64 x 64 = 4096 picture points covering 40 x 40 square arc min. The highest resolution is 1.5 arc min. for the unsmoothed display, and 2.25 arc min. after smoothing.

For the study of the radio bursts, most of the observation time will be spent for the fan-beam quick-scanning. But, when the sources are located ambiguously, a heliogram which is obtained by short interruption of the fan-beam scanning will play an important role to determine the source position unambiguously. For the monitoring of active regions, on the other hand, heliogram will play a leading role, especially when active regions are close to the limb where optical monitoring is difficult. This point is important for improving the forecasting of proton flares, which has been made at Toyokawa with one-dimensional interferometers.

It must also be remarked that the sensitivity of the existing 3-cm radioheliograph for active regions, which has been limited by short integration time, will be considerably improved by superposing several maps which will become available owing to the advent of a flexible control system and increased data-processing facility.

2. Overall System

The block diagram of the overall system is shown in Fig. 1. This system can be subdivided into several sections such as antenna system, receiving system, scanning device and small computer system, which are to be described separately in the following chapters. In this chapter, we briefly describe the overall system operation.

A general view of the antenna system is shown in Fig. 2. This picture is taken from the south. Part of the existing 3-cm radiohelio-

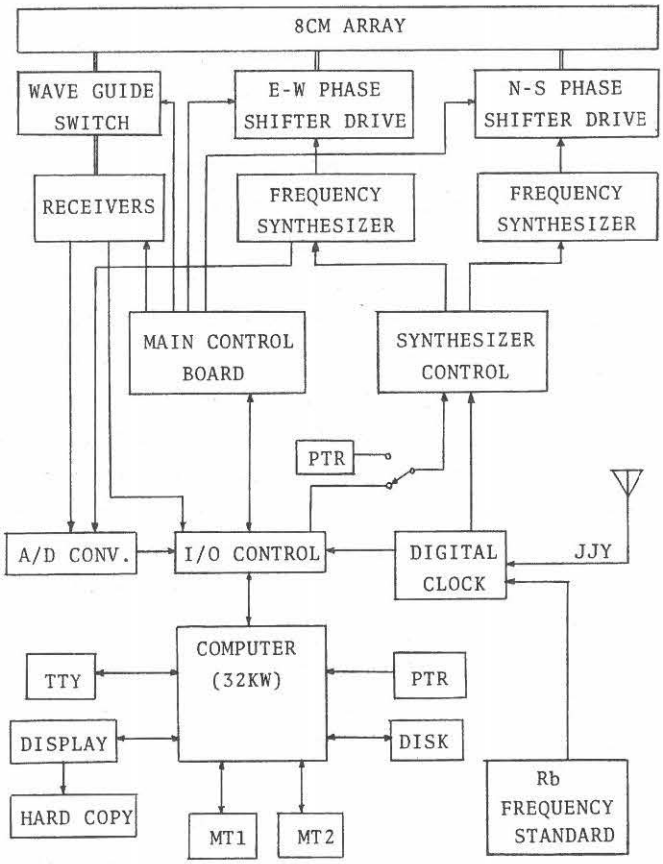

Fig. 1. Overall system block diagram.

graph is also seen on the left. Fig. 3 shows the geometrical configuration of the overall antenna system. The whole lengths of the array are 437 m in the E-W direction and 107 m in the N-S direction. The unit antenna spacing is about 6.88 m, which corresponds to 86.03 wavelengths. The grating lobe separation is more than 40 arc min., a little greater than the angular size of the radio sun. A step tracking system (Tanaka and Kakinuma 1965) cannot be used except for the observation by drift scanning.

The structure of the antennas and the transmission lines are quite the same as those described by Tanaka et al. (1969). The shape of the pencil beam is also given by Tanaka et al. (1970). The pencil beam formed by the T-shaped array is swept by the rotary phase shifters

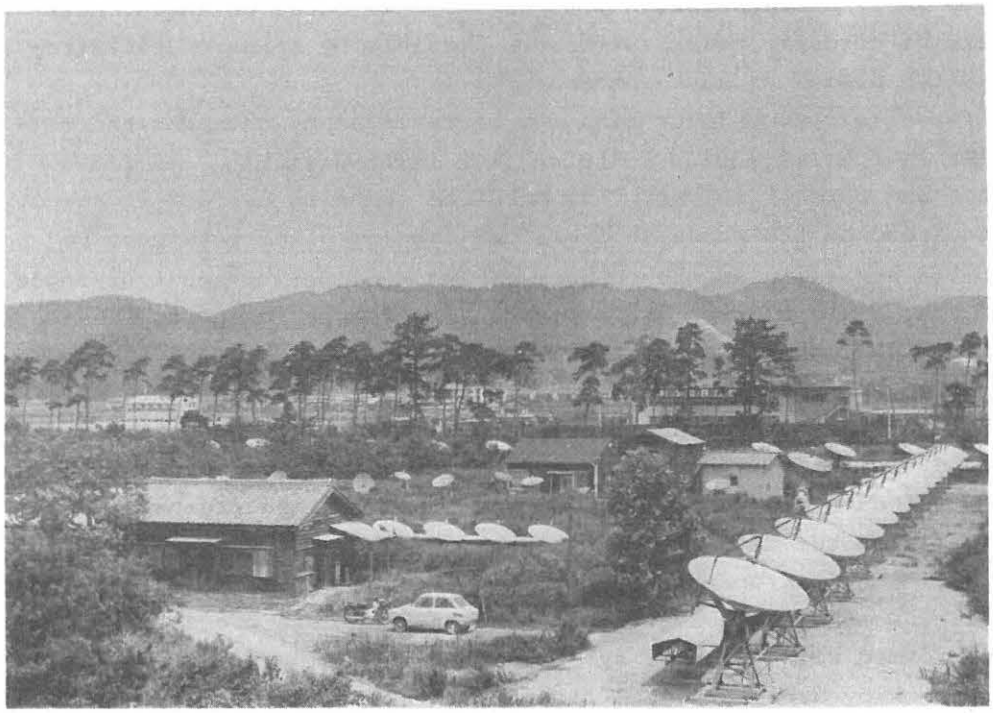

Fig. 2. A general view of 8-cm radioheliograph.

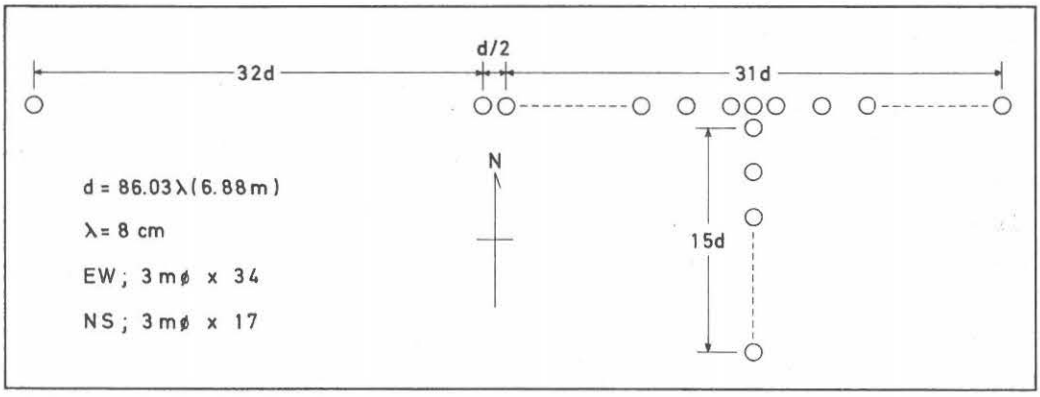

Fig. 3. Geometrical configuration of an array of 3mφ paraboloids.

equipped in each transmission line of the individual antennas. Measurements of circular polarization are possible by means of polarization switch placed on each antenna.

Different array configuration can be realized by changing the combination of four waveguide switches, two Dicke switches, two phase switches and three receivers. To make the scanning uniform in space, driving speed of the phase shifters and data sampling rate must be controlled according to the changes of the declination and hour angle of the sun. This control is performed precisely by changing the frequencies of two programmable frequency synthesizers by computer commands at an appropriate time interval.

Off-line control by punched paper tape is also possible in order that we do not miss important events when the computer system is down. The control data are composed of a pair of programmed frequencies and the times when the data are to be changed.

A real time disk operating system (RDOS) can manage the multi-job operation, so that data acquisition and on-line data processing are also performed with computer system. When the computer receives the interruption by a burst signal from the total flux observation, the running operational mode is automatically changed to the scanning mode of the highest speed.

In this way, the computer is being the pivot of this radioheliograph system, and it affords us much convenience in operating the rather complicated system.

3. Design of the Beam Scanning and Operational Modes

It is convenient to define the position of the sun with a pair of angles (θ, ϕ) rather than with the usual equatorial coordinates (δ, H), where θ is the angle measured from the meridian plane including the base line of N-S array, and ϕ is the angle from the vertical plane including the base line of E-W array. Relations between the above two coordinates are as follows;

$$\sin \theta = \cos \delta \sin H \ , \qquad (1)$$

$$\sin \phi = \sin \gamma \cos \delta \cos H - \cos \gamma \sin \delta \ , \qquad (2)$$

where γ is the latitude of the phase center of the T-shaped array, δ and H are the declination and hour angle of the sun.

As it is well known, the normalized power pattern of the T-shaped array is given by

$$P(\theta, \phi) = \frac{\sin nX}{n \sin X} \frac{\sin nY}{n \sin Y} \ , \qquad (3.a)$$

$$X = \pi (d/\lambda) \sin \theta \ , \qquad (3.b)$$

$$Y = \pi (d/\lambda) \sin \phi \ , \qquad (3.c)$$

where d is the unit spacing, λ is the operating wavelength, and n = 32 for our system.

It can be seen from Eqs. 3 that multiple responses are produced on the intersecting points of the two one-dimensional grating lobes. Let the orders of grating lobes for the E-W and N-S arrays be N and M respectively, which are sometimes called beam numbers, then the positions of the Nth and Mth fan beams are given as follows;

$$\sin \theta = (\lambda/d) N \ , \qquad (4)$$

$$\sin \phi = (\lambda/d) M \ . \qquad (5)$$

If we extend N and M from integers to decimals, the angular position (δ, H) can be expressed by (N, M) as shown in Fig. 4. The area surrounded by the dashed lines there indicates the sky coverage for solar observations, where the hour-angle coverage is limited by the receiver bandwidth. When the rotary phase shifters are driven, the E-W fan beams are swept from the west to the east, and the N-S fan beams from the south to the north. Consequently, a pencil-beam scanning can be controlled at a desired speed through the use of the E-W and N-S phase shifters independently. The normalized power pattern of the T-shaped array when it is being sweped by the rotary phase shifters is given by;

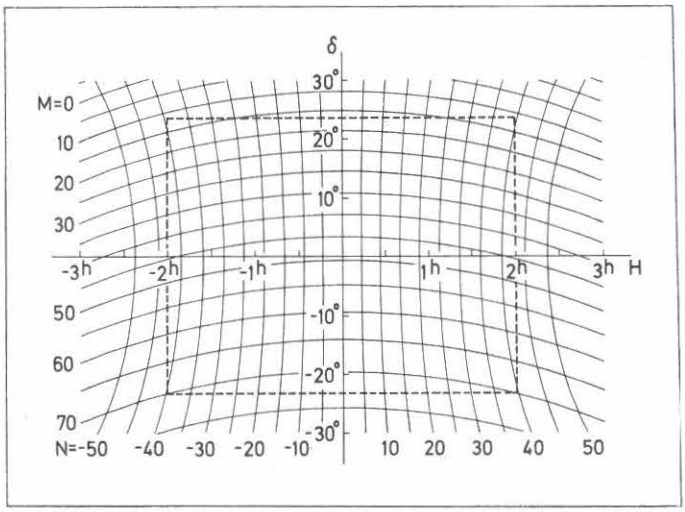

Fig. 4. Relations between the two coordinate system, (δ, H) and (N, M). The direction where N and M equal zero is the zenith.

$$P(\theta, \phi, t) = \frac{\sin nX'}{n \sin X'} \frac{\sin nY'}{n \sin Y'} , \tag{6.a}$$

$$X' = \pi [(d/\lambda) \sin \theta + f_{EW} (t - t_{EW})] , \tag{6.b}$$

$$Y' = \pi [(d/\lambda) \sin \phi + f_{NS} (t - t_{NS})] , \tag{6.c}$$

where f_{EW} and f_{NS} are the scanning frequencies in the two directions, and t_{EW} and t_{NS} are the times when the rotary phase shifters pass the standard positions. When $t = t_{EW}$ and at the same time $t = t_{NS}$, $P(\theta, \phi, t)$ is equal to $P(\theta, \phi)$, the position of the pencil beam coincides with that which is used for the transit system. In general,

if t_{EW} and t_{NS} are known, positions of the Nth and Mth fan beams are given as follows;

$$\sin \theta = (\lambda/d) \; [N - f_{EW} \; (t - t_{EW})] \; , \tag{7}$$

$$\sin \phi = (\lambda/d) \; [M - f_{NS} \; (t - t_{NS})] \; . \tag{8}$$

Using Eqs. 1, 2, 7, and 8, positions of the fan or pencil beams can be known relative to the center of the solar disk. Thus the design of the beam scanning in various fashions becomes possible.

We will show an example for the case of E-W fan-beam scanning. Let the position of the sun be $N_s(t)$ at the time of t. In order that a scan is finished after the time interval of ΔT, the following relation must be satisfied.

$$[N_s \; (t + \Delta T) - N_s \; (t)] + \int_t^{t + \Delta T} f_{EW} \; (t) \; dt = 1 \; . \tag{9}$$

From Eq. 9, f_{EW} (t) can be obtained as follows;

$$f_{EW} \; (t) = \frac{1}{\Delta T} - \frac{d \; N_s}{dt} = \frac{1}{\Delta T} - k \; s \; \cos \delta \; \cos \; (k \; t) \tag{10}$$

scans/sec., where k = H/t.

To make the scan interval constant irrespective of the rotation of the earth, the E-W phase shifters must be controlled according to Eq. 10. In our system, the scanning frequency is controlled digitally at an appropriate interval by a programmable frequency synthesizer. The control interval is determined so that the error may not exceed the tolerance limit. Other types of the scanning can be easily designed in the same manner as described above.

As shown in Table 1, there are six operational modes. Modes 1 and 2 are for the fan-beam scannings in two orthogonal directions, and modes

MODE	ARRAY CONFIGURATION	BEAM	SCANNING
1	EW32+, EW32xEW2, NS16+	FAN	QS
2	"	"	DS
3	T(EW32xNS16)	PENCIL	QS
4	"	"	DS
5	"	"	SS
PHASE CHECK	(EW16E+ EW16Ex17), (EW16W+ EW16Wx17), (NS16+ NS16x17)	FAN	QS, DS, SS

QS = Quick Scanning, DS = Drift Scanning, SS = Skip Scanning.

Table 1. Various operational modes of 8-cm array.

3, 4, and 5 are for the pencil-beam scanning. The type of the scanning is also classified into three kinds, quick scanning (QS), drift scanning (DS), and skip scanning (SS). When DS or SS is used, the E-W phase shifters are locked and the scanning in the E-W direction is performed only through the rotation of the earth. The SS mode has already been used sunce 1969 for the existing 3-cm radioheliograph. In the modes 1 and 2, fan-beam scannings are simultaneously performed with three interferometers, E-W 32-element grating interferometer (HPBW = 1.1 arc min.), E-W (32 + 2)-element compound interferometer (HPBW = 0.4 arc min.), and N-S 16-element grating interferometer (HPBW = 2.2 arc min.). Scan intervals are about 10 seconds for the mode 1, and 160 seconds for the mode 2.

In the modes 3, 4 and 5, pencil beams of the T-shaped array (HPBW = 2!3 x 2!3 cos ZD, ZD; Zenith Distance) are swept from the south to the north. For the mode 3, it takes about 40 seconds to complete a map, and for the mode 5, it takes about 20 minutes. It must be mentioned that, for the modes 2 and 5, simultaneous observations on the two wavelengths of 3 and 8 cm are possible.

Rotary phase shifter speeds, sample rates, mapping times, and number of picture points for each operational mode are summarized in Table 2. In Fig. 5 are illustrated the variations of the scan speed and the sam-

MODE	R_{EW}	R_{NS}	F_S	T	N
1	P=1	Q=1	25	10.24	256 (1 dim.)
2	0	Q=1	256/T	$1/k \cdot s \cdot \cos\delta \cdot \cos(k \cdot t)$	256 (1 dim.)
3	P=1	Q=64	100	40.96	4096 (2 dim.)
4	0	Q=64	4096/T	$1/k \cdot s \cdot \cos\delta \cdot \cos(k \cdot t)$	4096 (2 dim.)
5	0	Q=(8-1/8)8	4096/T	$8/k \cdot s \cdot \cos\delta \cdot \cos(k \cdot t)$	4095 (2 dim.)

$$R_{EW} = 465[P/T - k \cdot s \cdot \cos\delta \cdot \cos(k \cdot t)] \quad \text{(rpm)}$$

$$R_{NS} = 465[Q/T + k \cdot s \cdot \cos\delta \cdot \sin\gamma \cdot \sin(k \cdot t)] \quad \text{(rpm)}$$

$$F_S = N/T \quad (H_Z)$$

R_{EW} = EW rotary phase-shifter speed, R_{NS} = NS rotary phase-shifter speed, F_S = sample rate, T = mapping time(sec), N = number of picture points, γ = latitude, δ = declination, $k \cdot t$ = hour angle, $k = \pi/43200$, $s = 86.03$

Table 2. Rotary phase shifter speeds, sample rate, mapping time and the number of picture points for each operational mode.

ple rate against the hour angle of the sun. The upper left curve corresponds to Eq. 10. The curves in Fig. 5 depend slightly on the declination of the sun, so that the control values for the frequency synthesizers must be up-dated every day.

There are extra modes for checking the interferometer phasing through data processing. The method of phase correction which has been used for the compound interferometer can be applied also to the two-dimensional mapping of the sun (Ishiguro et al. 1972, Ishiguro 1974). For this purpose, an additional element is placed at the phase center of the T-shaped array. From simultaneous observations with the

16-element grating interferometer and the (16 + 1)-element compound interferometer for each of the three arms of the array, phase errors of the antennas can be estimated by the above method. It is only through the correction of the phase error for each Fourier component that a refined radio map of the sun can be obtained.

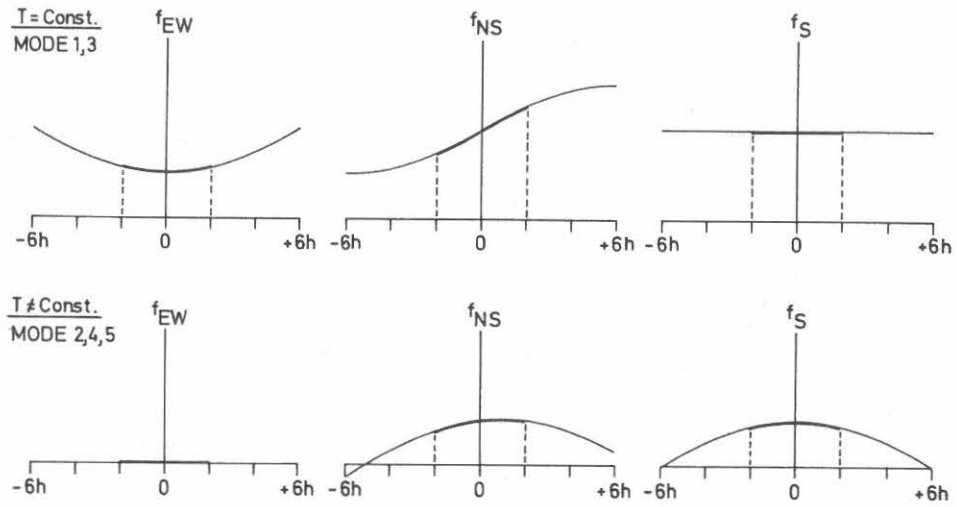

Fig. 5. Variations of scan speeds and the sample rate with hour angle (f_{EW}; E-W scan speed, f_{NS}; N-S scan speed, f_S; sample rate).

4. Phase Shifter Driving System

The rotary phase shifters for the new 16-element N-S array are substantially similar to those for the existing E-W grating and compound interferometers (Tanaka et al. 1969). They are continuously driven through the sixteen kinds of gearing which are coupled to a common shaft, so as to give a linear phase shift along the array. Consequently, a control of the scanning speed is performed only through the common shaft.

As shown in Fig. 6, there are two phase shifter drive systems; one

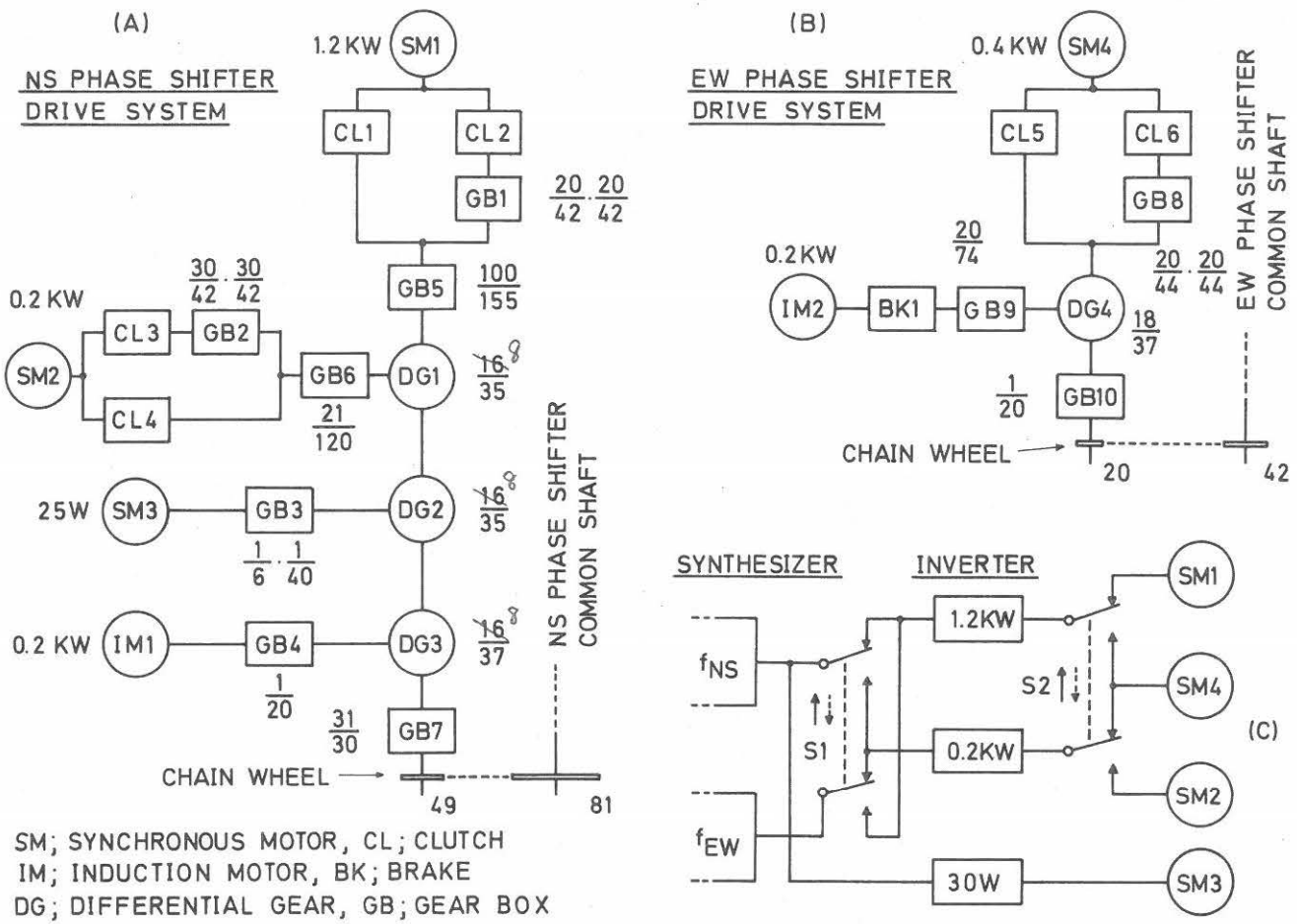

Fig. 6. Phase shifter drive system.

for the N-S and the other for the E-W common shaft. These systems are rather complicated in order to cover the extensive range of the operating speed. Three 3-phase inverters, controlled by a pair of frequency synthesizers, drive four synchronous motors for the precise control of rotary phase shifters. The range of the driving speed of the phase shifters is extended by changing the gear ratio of the driving system. Various states of the clutches (CL1 ∿ CL6), brake (BK1) and switches (S1 and S2) are given for each operational mode in Table 3.

The rotational speed of the N-S common shaft must be varied from 1.5 rpm to 727.4 rpm through all modes. On the other hand, the corresponding value for the E-W common shaft ranges from 8.4 rpm to 43.1 rpm. There are also equipments for each drive system which generate a pulse-train. Each pulse interrupts the computer to record and store the time when the rotary phase shifter has passed a standard position with which the angular position of the beam can be determined.

Induction motors in Fig. 6 are used to stop the phase shifters at the standard position when the synchronous motors are switched off.

MODE	CL1	CL2	CL3	CL4	CL5	CL6	BK1	S1	S2
1	1	1	0	1	1	0	1	↓	↓
2	1	1	1	1	0	0	0	-	-
3	1	0	1	1	0	1	1	↑	↑
4	0	1	1	1	-	-	-	↑	↑
5	1	1	1	0	-	-	-	↓	↓

(ON.....1, OFF.....0.)

Table 3. Combination of clutches, brake and switches in the phase shifter drive system for each operational mode.

5. Transmission Lines and Receiving System

Fig. 7 shows simplified relations among antennas, transmission lines, waveguide switches, Dicke switches, phase switches and receivers. Transmission lines for the new 17-element N-S array are made quite similar to those for the E-W array (Tanaka et al. 1969) in order to equalize the total electrical length from each feed to the receiver. The total transmission loss is about 4 dB. Waveguide switches and the front ends of the receivers are placed at the center of the 32-element E-W array as shown in Fig. 9. A different array configuration must be formed to change the operational mode as described in Chapter 3. Four waveguide switches of two different types are prepared to change or combine the flow of microwave signal from each array. One consists of two corners (LL) and another consists of a magic-T and a corner (TL). The actual structure of the latter is shown in Fig. 10. These rotary waveguide switches automatically stop at correct positions when an operator gives command for a certain operational mode either from the control panel or from the teletypewriter. In Fig. 8, the positions of waveguide switches are shown for each operational mode.

Thus the microwave signals are combined and transmitted to the three receivers, R1, R2 and R3. The selection of these receivers is shown in the table of Fig. 7. The system has also two phase switches PS1 and PS2, and two Dicke switches DS1 and DS2. The phase switch consists of a turnstile and a $\pm 45°$ gyrator, of which Kakinuma and Tanaka (1963) already described. The insertion loss is about 0.7 dB. A different type of ferrite switch shown in Fig. 11 is used for the Dicke switch. It can alternately switch the ports 1 and 2 at an increased speed of 5 KHz to adapt for the high-speed scanning. In some cases, the microwave signals will be transmitted through both phase and Dicke switches. When one of them is unnecessary for the operation, a constant DC current is applied.

A block diagram of the receiving system is shown in Fig. 12. The radio frequency section is composed of a tunnel-diode amplifier (TDA), a image-rejection filter, a mixer preamplifier and a local oscillator. The noise figure and the gain of TDA is 4.5 dB and 20 dB respectively. the local oscillator consists of a crystal-controlled oscillator and a varactor frequency multiplier, which produces a stabilized signal at around 3778.5 MHz.

The IF amplifier has the ability of variable bandwidth, 0.5, 1, 2, 5 and 10 MHz, with the center frequency of 30 MHz and the gain of 30 dB. The gain of the receiver can be controlled both by an automatic level control (ALC) and a step attenuator. The ALC is a 4-bit pin-diode attenuator which gives attenuation from 0 dB to 45 dB with

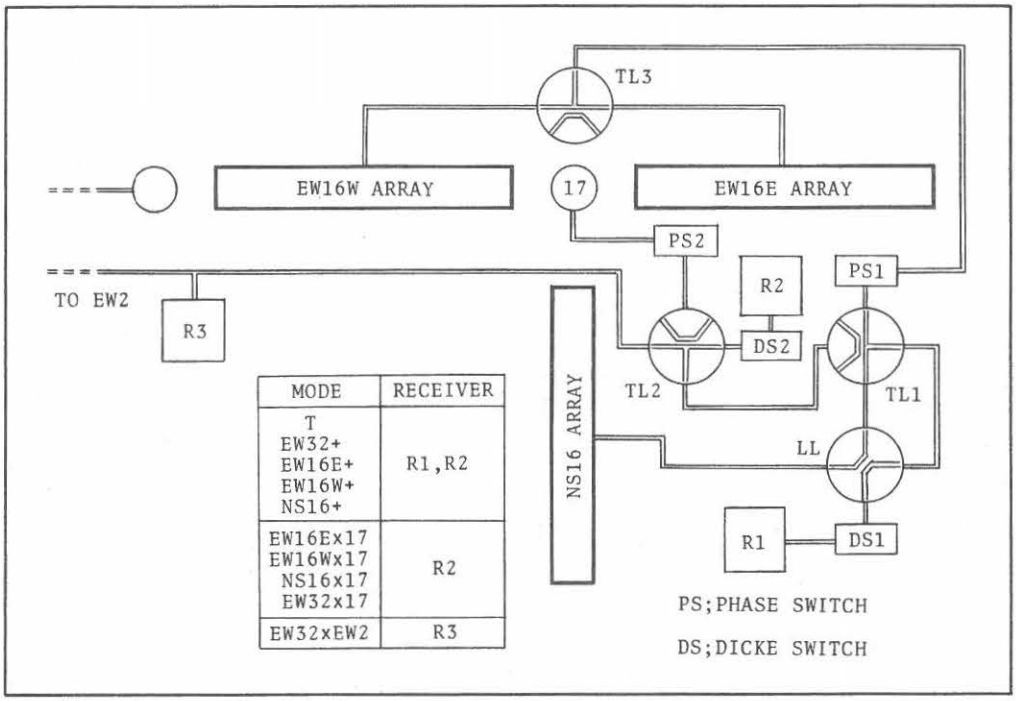

Fig. 7. Transmission lines and the receiving system.

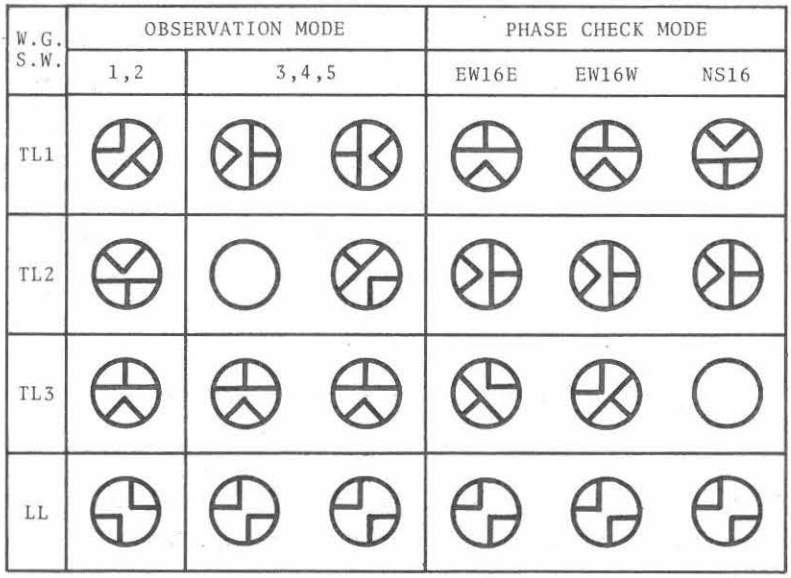

Fig. 8. Combinations of the positions of waveguide switches.

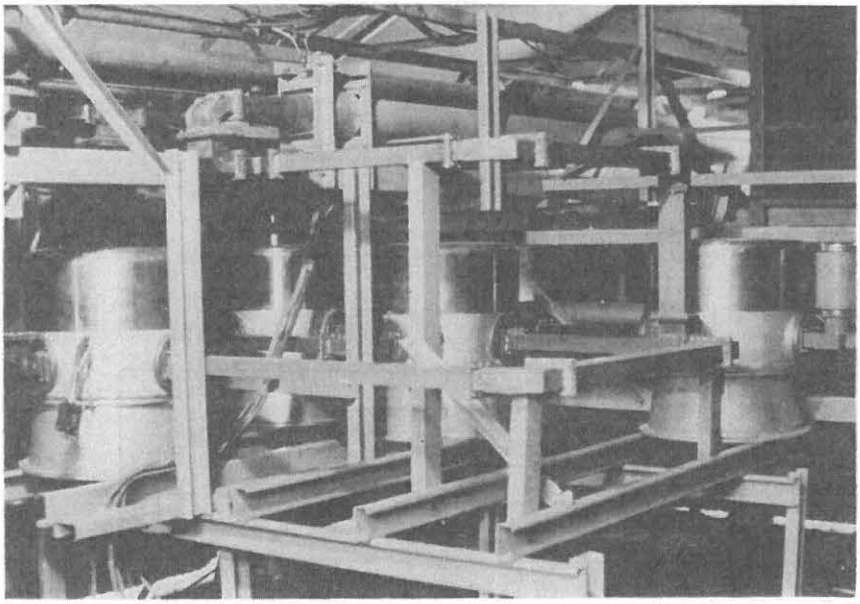

Fig. 9. An outside view of the waveguide switches in a small house placed at the phase center of the T-shaped array.

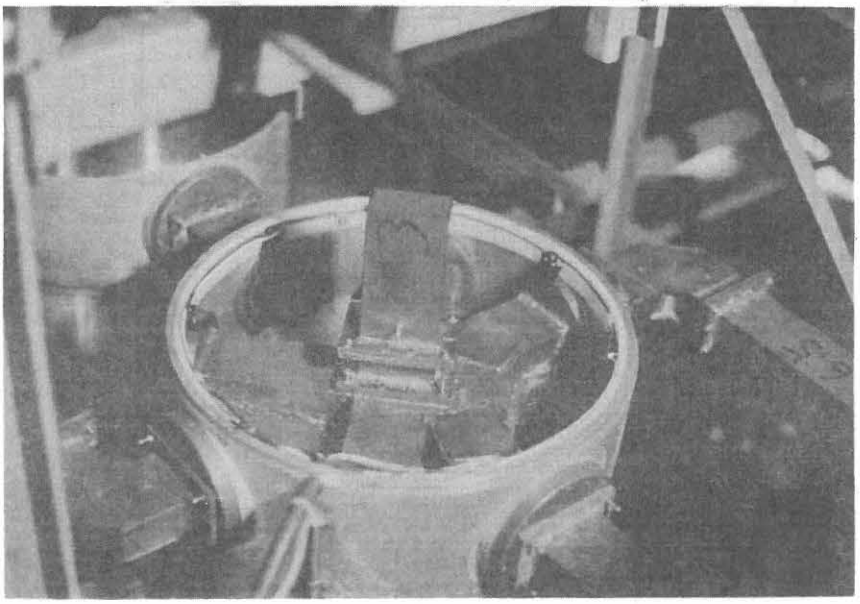

Fig. 10. An example of the structure of a waveguide switch.

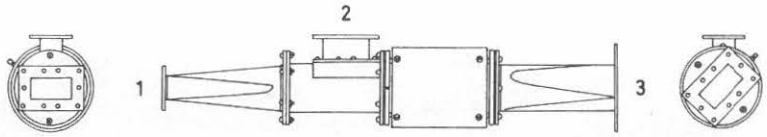

Fig. 11. A ferrite switch for the Dicke switching.

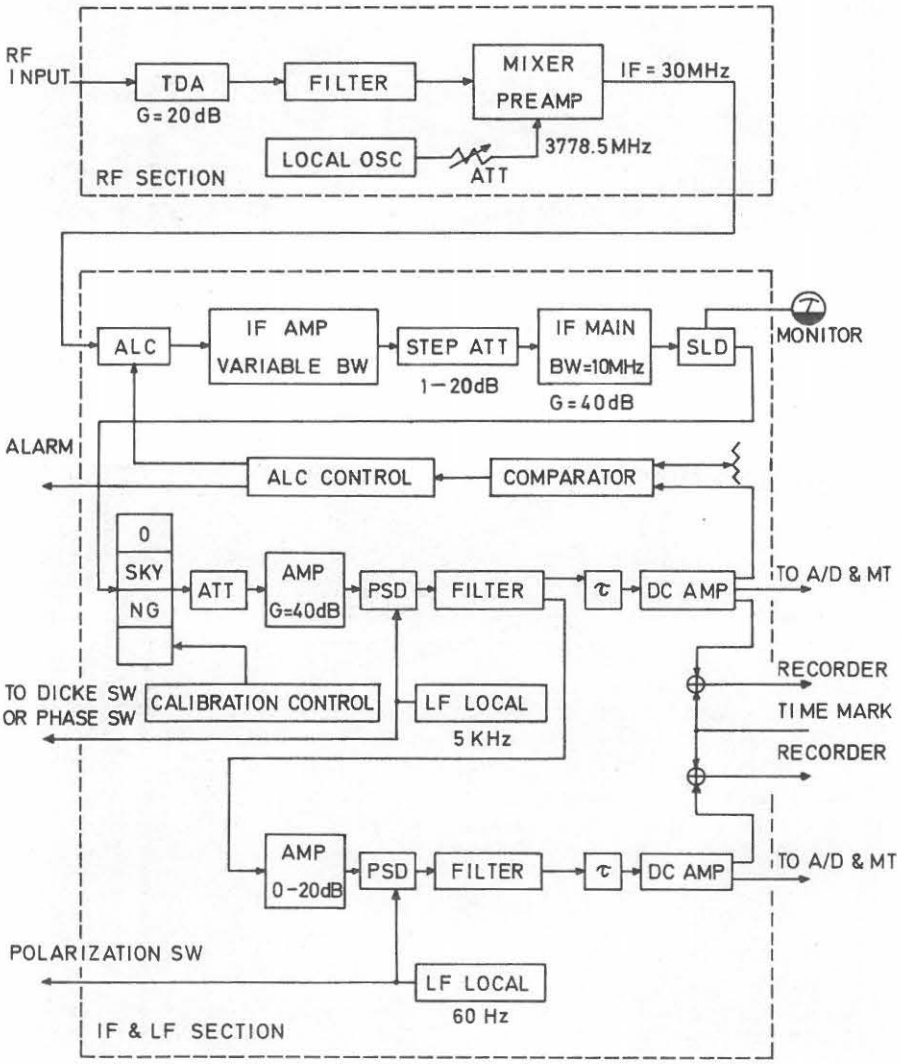

Fig. 12. A block diagram of the receiver.

3 dB increment. This 4-bit code is always recorded with digitized receiver outputs.

After the square-law detector, the signal passes through the conventional LF section, where it is synchronously detected by the reference signal, integrated, and then amplified to drive a chart recorder and an A/D converter. The over-all receiver gain is calibrated by a noise tube and the sky temperature. The IF and LF sections are placed in a temperature-controlled room, together with the existing receivers and the computer facilities.

6. Control, Data Acquisition and Data Processing

As shown in Fig. 1, various functions of the radioheliograph system are controlled by a small on-line computer system. The computer consists of a 16 bit, 1.2-μs CPU with 32 K words of core memory and a hardware floating-point and multiply/divide processors. As peripheral equipments, the system has 1.2 M words, 2200 BPI moving-head disk, two

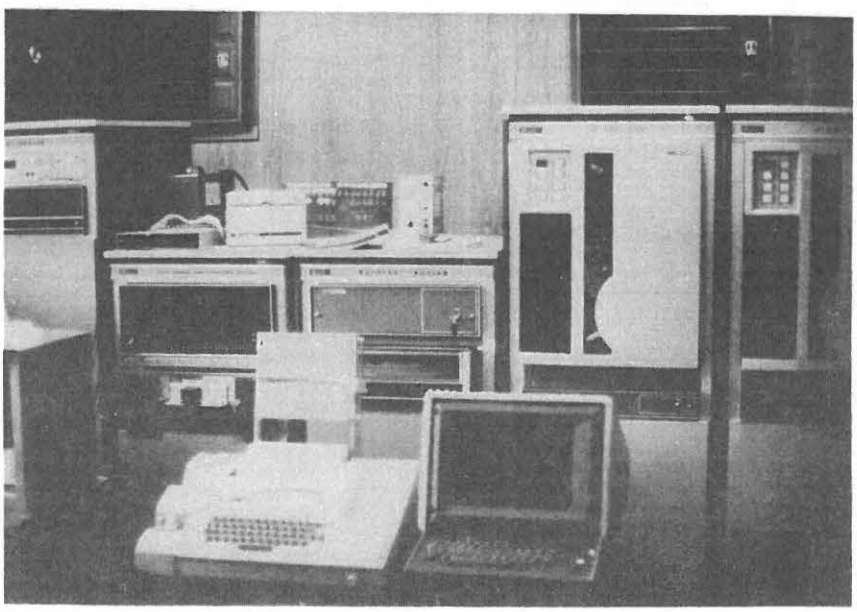

Fig. 13. A general view of the computer system.

2 IPS, 800 BPI, 9 track magnetic tapes, a high speed paper-tape reader, ASR-33 teletypewriter, a graphical and alphanumeric display unit (Tektronix 4010) with its hard copy unit, a digital clock controlled by a Rb frequency standard and a 12-bit 8-channel A/D converter. A general view of the computer system is shown in Fig. 13. Under normal operation, one magnetic-tape transport is used to write data as a foreground use, but the other transport is available to the background users for data processing. A multi-purpose I/O control is built to interface the main control board, synthesizer controller, A/D converter, digital clock, and other auxiliary equipments.

The system is supported by a real-time disk-operating system (RDOS), which enables the simultaneous operation of the foreground and background jobs. The foreground job can be divided into mode setting, synthesizer control and data acquisition; and the background job into control data generation, monitering, data processing and display. Programming by FORTRAN language is available for the background job. The relations between these tasks are shown in Fig. 14. The contents of these tasks are described below.

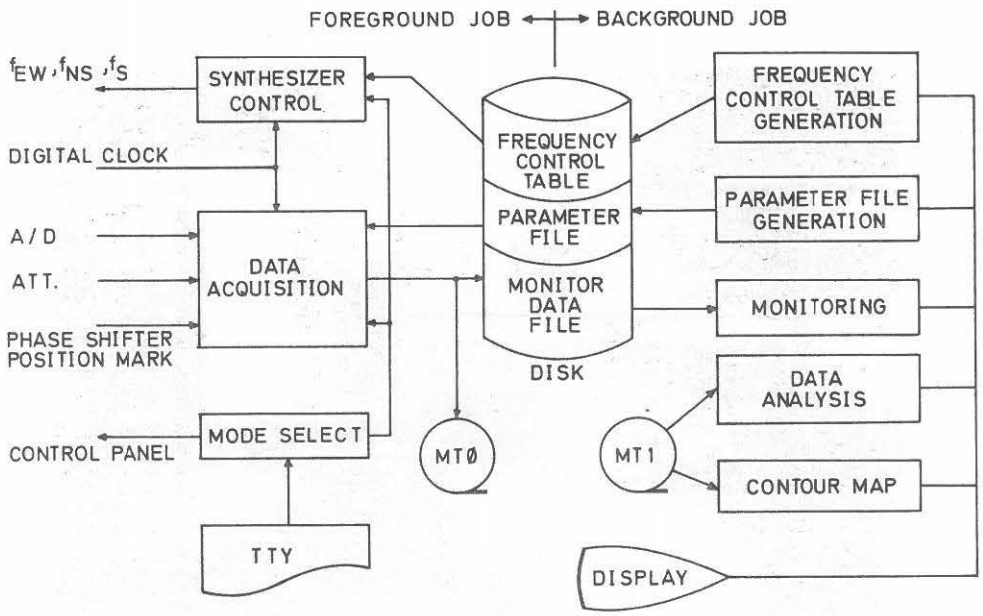

Fig. 14. A simplified flow diagram of the computer system.

6.1 Control Data Generation

Before starting the observation, control data for each oprational mode must have been generated on the magnetic-disk file. These data consist of a frequency control table for the synthesizer controller and the parameter file which specifies the sampling rate for each A/D converter channel and the related attenuater number. These control data generation jobs are carried out by an operator on the background graphical and alphanumeric display console.

The contents of the frequency control table are quite the same as those for the punched paper tape that is to be used in the off-line synthesizer control. These control data files are stored with the data and the starting time of the observation in the foreground magnetic tape, before starting the data acquisition for use in the stage of the data reduction.

6.2 Mode Setting and Synthesizer Control

Mode setting is carried out through the main control board. So, the computer has only to transfer the message to the board. When the operator starts the foreground program, the computer asks the date and operational mode, then the operator selects one specified mode and answer the question by on-line teletypewriter. The computer, soon after, starts the control program and transfers the 16- bit code about the operational mode to the main control board.

A simplified function of the main control board is shown in Fig. 15. Commands for the start, stop and mode selection of the system can be given both through the main control board and the on-line teletypewriter. The computer picks up from the frequency-control table a set of programmed times and frequencies corresponding to the selected mode, and transfers it to the synthesizer controller (Fig. 16) one after another when the real time on the digital clock gets a coincidence with the programmed time. The frequency and time are controlled at the precisions of 1 mHz and 10 msec. respectively. Reversible counters in Fig. 16 are to be used for the digital feedback control of the phase shifter speeds. When the system is interrupted by a burst signal, the operational mode is automatically changed to the 'mode 1', and at the same time an analog magnetic tape starts to make sure the recording.

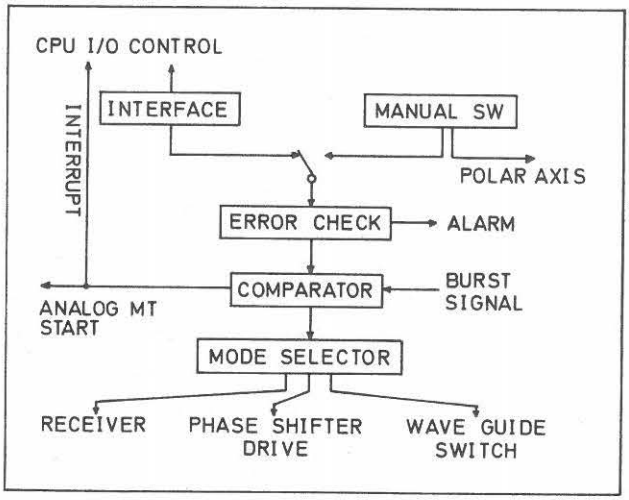

Fig. 15. Functions of the main control board through which system control is performed.

6.3 Data Acquisition, Monitoring and Data Processing

As shown in Fig. 14, data inputs to the computer are the digitized receiver outputs (11 bit), status information on the attenuators (4 bit) and the time when the rotary phase shifter passes through a specified position (position mark in Fig. 14).

An A/D converter has eight multiplexer channels for analog inputs and has a minimum conversion time of 33 μs. The 11 bit data plus one sign bit from each channel are packed with the 4-bit attenuator status code to be stored in the CPU buffer memory as one word (= 16 bit). these are unpacked and reconstructed to the original value in the stage of the data reduction. Data sampling rate is fixed or varied with time according to the operational mode.

There will also be some differences among the sampling intervals for each multiplexer channel. But, those intervals, which are programmed in the parameter file, should be the integral multiples of the fundamental unit. The maximum and minimum sampling rate are 100 Hz and 1.2 Hz respectively. At the maximum sampling rate, a reel of 1200-ft magnetic tape should be renewed day after day!

A unit CPU buffer memory has the size of 128 words. Usually each

data channel has a pair of unit buffer memories for the switching use. After the blocking of the data into a unit of 128 words is completed, these data blocks are immediately stored on the magnetic tape. Times of the data acquisition are also attached to them. As it is necessary to monitor the observed data as soon as possible, these data are also stored on the monitor data file (80 k words) on the disk, which can be read out from a background monitoring program at any desired time.

The size of the foreground job including the operating system is about 12 K words. The remaining 20 K words are available for the monitoring and data processing as a background job. There will be many kinds of data processing such as the sorting and/or the editting of the data on magnetic tapes, calibrations including the phase error correction, a statistical processing so as to produce a clean map, and so on. The same kind of data observed with the existing 3-cm radio-heliograph are also processed with this computer.

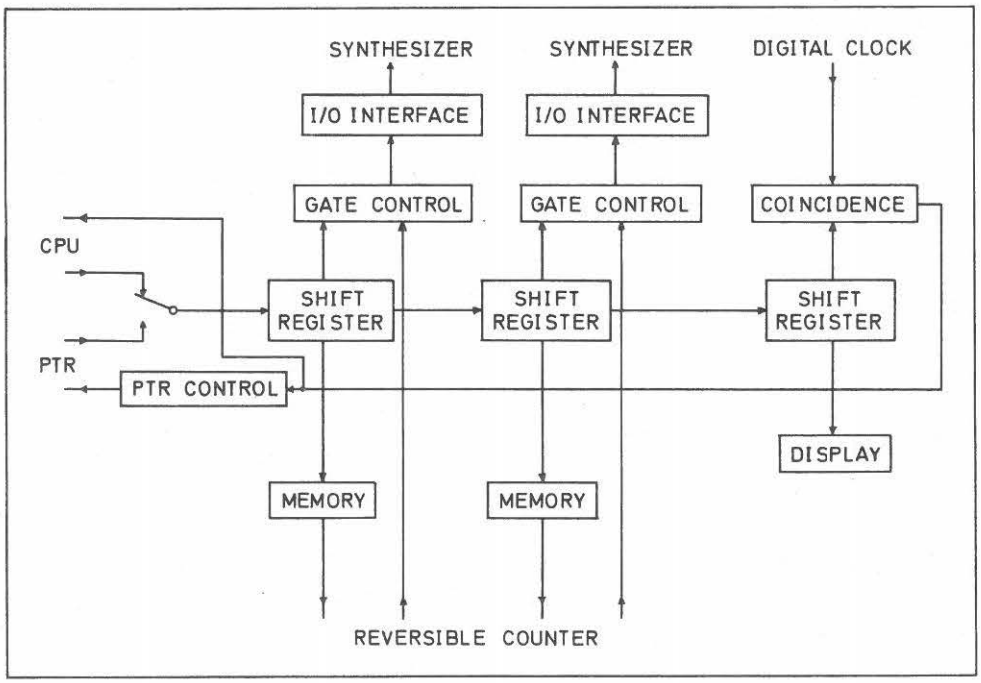

Fig. 16. Synthesizer controller. Control data are being stored on three 8-byte shift registers, untill the programmed time coincides with the real time.

Making the most of the graphical and alphanumeric display unit in an interactive manner, the level of efficiency of the data reduction should be raised. A detailed explanation on the data processing will be published in a separate paper.

References

Arisawa, M.: Improved Radio Mapping of the Sun, Proc. Res. Inst. Atmospherics, Nagoya Univ., 18, 89 (1971).

Enome, S., T. Kakinuma and H. Tanaka: High-Resolution Observations of the Solar Radio Burst with Multi-Element Compound Interferometers at 3.75 and 9.4 GHz, Solar Phys., 6, 428 (1969).

Enome, S. and H. Tanaka: Magnetic Fields in the Lower Corona Associated with the Expanding Limb Burst on March 30th 1969 inferred from the Microwave High-Resolution Observations, Solar Magnetic Fields, 413, IAU (1971).

Enome, S. and H. Tanaka: Structure of Proton Centers and Associated Nonthermal Burst at Microwave Frequencies, High Energy Phenomena on the Sun, NASA SP-342 (1973).

Ishiguro, M.: Image Correction in High-Resolution Radio Interferometer, Proc. Res. Inst. Atmospherics, Nagoya Univ., 18, 73 (1971).

Ishiguro, M., S. Enome and H. Tanaka: A New Project of 8-CM Radioheliograph, Proc. Res. Inst. Atmospherics, Nagoya Univ., 19, 105 (1092).

Ishiguro, M.: Phase Error Correction in Multi-Element Radio Interferometer by Data Processing, Astron. Astrophys. Suppl. 15, 431 (1974).

Swarup, G., T. Kakinuma, A.E. Covington, G.A. Harvey, R.F. Mullay and J. Rome: High-Resolution Studies of Ten Solar Active Regions at Wavelengths of 3 - 21 CM, Ap. J., 137, 4, 1251 (1963).

Tanaka, H, and T. Kakinuma: Preliminary Results of Observations of the Source of Slowly Varying Component with Two Interferometers at 9400 and 4000 Mc/s, Proc. Res. Inst. Atmospherics, Nagoya Univ., 7, 79 (1960).

Tanaka, H. and T. Kakinuma: The Relation Between the Spectrum of Slowly Varying Component of Solar Radio Emission and Solar Proton Event, Rep. Ionosph. Space Res. Japan, 18, 1, 32 (1964).

Tanaka, H. and T. Kakinuma: Improvement of the High-Resolution Interferometer at 9.4 Gc/s, Proc. Res. Inst. Atmospherics, Nagoya Univ., 12, 27 (1965).

Tanaka, H., T. Kakinuma and S. Enome: High-Resolution Observations of the Sources of Solar Radio Burst at 9.4 Gc/s, Proc. Res. Inst. Atmospherics, Nagoya Univ., 14, 23 (1967).

Tanaka, H., T. Kakinuma, S. Enome, C. Torii, Y. Tsukiji and S.Kobayashi: A High-Resolution Quick-Scan Interferometer for Solar Studies at 3.75 GHz, Proc. Res. Inst. Atmospherics, Nagoya Univ., 16, 113 (1969).

Tanaka, H., T. Kakinuma and S. Enome: The Slowly Varying Component of the Radio Emission during the Period of July 1966 Proton Flare, Annals of IQSY, 3, 63, MIT Press (1969).

Tanaka, H., S. Enome, C. Torii, Y. Tsukiji, S. Kobayashi, M. Ishiguro and M. Arisawa: 3-CM Radioheliograph, Proc. Res. Inst. Atmospherics, Nagoya Univ., 17, 57 (1970).

Tanaka, H. and S. Enome: High-Resolution Observations of Solar Microwave Bursts, Nature, 225, Jan. 31, 435 (1970).

Tanaka, H. and S. Enome: The Microwave Structure of Coronal Condensations and its Relation to Proton Flares, Solar Phys., 40, 1, 271 (1975).